Available online at www.sciencedirect.com
ScienceDirect
Journal of Power Sources 160 (2006) 37–43
JOURNAL OF POWER SOURCES
www.elsevier.com/locate/jpowsour

Investigation of ethanol electrooxidation on a Pt–Ru–Ni/C catalyst for a direct ethanol fuel cell

Zhen-Bo Wang *, Ge-Ping Yin, Jian Zhang, Ying-Chao Sun, Peng-Fei Shi

Department of Applied Chemistry, Harbin Institute of Technology, Harbin, China 150001

Received 31 October 2005; received in revised form 24 December 2005; accepted 5 January 2006
Available online 13 February 2006

Abstract

This research is aimed to improve the utilization and activity of anodic alloy catalysts and thus to lower the contents of noble metals and the catalyst loading on anodes for ethanol electrooxidation. The DEFC anodic catalysts, Pt–Ru–Ni/C and Pt–Ru/C, were prepared by a chemical reduction method. Their performances were tested by using a glassy carbon working electrode and cyclic voltammetric curves, chronoamperometric curves and half cell measurement in a solution of 0.5 mol L^{-1} CH_3CH_2OH and 0.5 mol L^{-1} H_2SO_4. The composition of the Pt–Ru–Ni and Pt–Ru surface particles were determined by EDAX analysis. The particle size and lattice parameter of the catalysts were determined by means of X-ray diffraction (XRD). XRD analysis showed that both of the catalysts exhibited face centered cubic structures and had smaller lattice parameters than a Pt-alone catalyst. Their particle sizes were small, about 4.5 nm. No significant differences in the ethanol electrooxidation on both electrodes were found using cyclic voltammetry, especially regarding the onset potential for ethanol electrooxidation. The electrochemically active specific areas of the Pt–Ru–Ni/C and Pt–Ru/C catalysts were almost the same. But, the catalytic activity of the Pt–Ru–Ni/C catalyst was higher for ethanol electrooxidation than that of the Pt–Ru/C catalyst. Their tolerance to CO formed as one of the intermediates of ethanol electrooxidation, was better than that of the Pt–Ru/C catalyst.

Keywords: Direct ethanol fuel cell; Pt–Ru–Ni/C catalyst; Pt–Ru/C catalyst; Ethanol electrooxidation

1. Introduction

The direct methanol fuel cell (DMFC) uses aqueous or gaseous methanol directly and without prior complicated reforming. The structure of the DMFC is simple. The DMFC has been receiving increased attention due to its advantages of easy transportation and storage of the fuel, reduced system weight, size and complexity, and its high energy efficiency [1–3]. However, methanol has some disadvantages, for example, it is relatively toxic, has a low boiling point (65 °C), and is not a primary fuel. Therefore, other alcohols are being considered as alternative fuels [4]. Ethanol is an interesting and attractive fuel for electric vehicles, mobile telephone and laptops. Ethanol is not toxic and less volatile. It is inexpensive and easily transported. It can be easily produced in great amounts by fermentation. So, proton exchange membrane fuel cells (PEMFC) using ethanol as a fuel have been studied [5,6]. The oxidation of ethanol is more difficult than that of methanol with the necessity of breaking the C–C bond for complete oxidation. To increase the electroactivity of ethanol is a crucial task, and together with its complete oxidation into carbon dioxide, it is a hard challenge [7]. Platinum itself is known to be rapidly poisoned at its surface by strongly adsorbed species coming from the dissociation of organic molecules. So, the anodic current from ethanol electrooxidation on Pt is very sluggish, especially at low temperatures. There is a need to improve the activity of catalysts for ethanol electrooxidation. The only possible way is to modify the electrode surface in order that, at low potentials, its coverage of oxygenated species (e.g. adsorbed OH) from the dissociation of water is increased. These OH species are necessary to oxidize completely to carbon dioxide, the species from the dissociation of ethanol. The number of possible metals which are able to activate water at a lower potential with a sufficient stability in acid medium is rather limited. Pt–Ru alloys are still considered

* Corresponding author at: Department of Applied Chemistry, Harbin Institute of Technology, No. 92, West Da-Zhi Street, Harbin, China.
Tel.: +86 451 86402571; fax: +86 451 86402576.
E-mail addresses: wangzhenbo1008@yahoo.com.cn, wangzhb@hit.edu.cn (Z.-B. Wang).

0378-7753/$ – see front matter © 2006 Elsevier B.V. All rights reserved.
doi:10.1016/j.jpowsour.2006.01.021

to be the best catalysts, because of their tolerance to CO, and are widely used in DMFCs [8]. The performance of a binary Pt–Ru alloy catalyst for ethanol electrooxidation is not the best [9]. Furthermore, platinum and ruthenium are noble metals. The resources of platinum are limited, and that of ruthenium is scarce. So, it is worth studying a base metal that may be used as an additional metal in the anodic catalyst for the direct ethanol fuel cell (DEFC). It may lower its cost, and accelerate industrialization.

The addition of a third metal (Mo or Sn) improves the performance of the electrode [10,11], but its stability with time needs further improvement. Theoretical calculations have shown that the segregation processes that generally lead to Pt surface enrichment are unlikely to occur in the Pt–Ni system [12]. Furthermore, in the potential range, at which the alcohol electrooxidation proceeds, Ni from the Pt–Ni alloy would not dissolve in the electrolyte, while Ru would dissolve out of the Pt–Ru alloy. The resistance to dissolution has been attributed to a nickel hydroxide passivated surface, thus enhancing the stability of Ni in the Pt lattice [13]. Despite these apparent advantages, carbon supported Pt–Ni systems such as for DMFC anodes were studied only a little [14]. The direct methanol electrooxidation on nickel based (Pt–Ni) thin film and alloy (Pt–Ru–Ni) nanoparticles as anode catalysts has been reported [13,15]. The use of Pt–Ni systems as DMFC cathodes has been much investigated [16–20]. But, these catalysts were alloy powders, and not supported on carbon. At present, the use of carbon supported Pt–Ru–Ni systems as DEFC anodes remains relatively unexplored. Based on these literature findings, we think it meaningful to explore the carbon supported Pt–Ru–Ni catalysts prepared by chemical reduction for DEFCs. We have investigated ethanol electrooxidation on these catalysts. The performance of the Pt–Ru–Ni/C catalyst was compared with that of a Pt–Ru/C catalyst obtained by chemical reduction of H_2PtCl_6 and $RuCl_3$ as precursors with sodium borohydride.

2. Experimental

2.1. Preparation of catalysts

The carbon black powder (Vulcan XC-72, Cabot) was used as a support for the catalyst. All the samples contained 20% metal in weight of the catalyst. 0.25 g Pt–Ru (with an atomic ratio of 1:1)/C or Pt–Ru–Ni (with an atomic ratio of 6:3:1)/C catalyst was obtained by chemical reduction [21] with sodium borohydride of H_2PtCl_6, $RuCl_3$ and $NiCl_2$ as precursors at 80 °C. The carbon black was ultrasonically dispersed in a mixture of ultra-pure water and isopropyl alcohol for 20 min. The precursors were added to the ink and then mixed thoroughly for 15 min. The pH value of the ink was adjusted by NaOH solution to 8 and then raised its temperature to 80 °C. Twenty-five milliliters of 0.2 mol L^{-1} solution of sodium borohydride was added into the ink drop by drop, and the bath was stirred for 1 h. The mixture was cooled, dried and washed repeatedly with ultra-pure water (18.2 MΩ cm) until no Cl^- ions existed. The catalyst powder was dried for 3 h at 120 °C and stored in a vacuum vessel. All chemicals used were of analytical grade.

2.2. Preparation of working electrode and its electrochemical measurements

2.2.1. Preparation of working electrode

Three millimeter diameter glassy carbon working electrodes (electrode area 0.0706 cm^2), polished with 0.05 μm alumina to a mirror-finish before each experiment, were used as substrates for the Vulcan-supported catalysts. For the electrode preparation, 5 μL of an ultrasonically redispersed catalyst suspension was pipetted on to the glassy carbon substrate. After the solvent evaporation, the deposited catalyst (28 $\mu g_{metal}\ cm^{-2}$) was covered with 5 μL of a dilute aqueous Nafion solution (5 wt.%). The resulting Nafion film with a thickness of ≤0.2 μm had a sufficient strength to attach the Vulcan particles permanently to the glassy carbon electrode without producing significant film diffusion resistances [22].

2.2.2. Preparation of half-cell

The diffusion electrodes were prepared for the investigation of the electrochemical oxidation of ethanol. First, the Pt–Ru/C or Pt–Ru–Ni/C catalyst was suspended in Millipore conductivity water and agitated in an ultrasonic bath for 30 min. Subsequently, the slurry was mixed with perfluorosulfonic acid solution (5 wt.%, Nafion, Du Pont), ethylene glycol and acetylene black (10 wt.%) by ultrasonic agitation for 1 h. The obtained catalyst ink was spread on a carbon paper (Toray). The metal loading in the electrode was 2.0 mg cm^{-2}. The half-cell was finally made by hot-pressing the anode on one side of a pretreated Nafion-117^{TM} membrane under a pressure of 50 kg cm^{-2} at 130 °C for 3 min. The half-cell so formed was typically with a thickness of about 0.7 mm. The apparent area of the half-cell is 1 cm^2.

2.2.3. Electrochemical measurements

Electrochemical measurements were carried out with a conventional three-electrode electrochemical cell at 25 °C. The glassy carbon electrode as the working electrode (electrode area 0.0706 cm^2) was covered with the catalyst powder. A piece of Pt foil of 1 cm^2 area was used as the counter one. The reversible hydrogen electrode (RHE) was used as the reference one with its solution connected to the working electrode by a Luggin capillary. All potential values are versus RHE. All chemicals used were of analytical grade. All the solutions were prepared with ultra-pure water (MilliQ, Millipore, 18.2 MΩ cm). A solution of 0.5 mol L^{-1} CH_3CH_2OH and 0.5 mol L^{-1} H_2SO_4 was stirred constantly and purged with ultra-pure argon gas. Electrochemical experiments were performed by using a CHI630A electrochemical analysis instrument. Cyclic voltammograms (CV) was plotted within a potential range from 0.05 to 1.2 V with a scanning rate of 0.02 V s^{-1}. The chronoamperometric experiments were carried out by using CHI630A electrochemical analysis instrument controlled by an IBM PC. The potential jumped from 0.1 to 0.8 V. Due to a slight contamination from the Nafion film, the working electrodes were electrochemically cleaned by continuous cycling at 0.05 V s^{-1} until a stable response was obtained before the measurement curves were recorded.

2.2.4. Half-cell measurements

Half-cell measurements were carried out with a two-compartment cell at 25 °C. The half-cell as a working electrode with an area of 1 cm^2 was put in the left compartment with a solution of 0.5 mol L^{-1} CH_3CH_2OH and 0.5 mol L^{-1} H_2SO_4. A piece of Pt foil of 1 cm^2 area was used as the counter one and put in the right compartment with a solution of 0.5 mol L^{-1} H_2SO_4. The reversible hydrogen electrode was used as the reference one with its solution connected to the working electrode by a Luggin capillary. Anode polarization curves of the Pt–Ru–Ni/C or Pt–Ru /C electrode during the electrooxidation of ethanol were recorded under quasisteady state conditions as a function of potential (E), that is, $i(E)$ curves (i being measured and calculated after 5 min at each potential).

2.2.5. CO stripping voltammetry

The electrode was electrochemically cleaned in an Ar-degassed solution of 0.5 mol L^{-1} H_2SO_4 at 25 °C. The amount of the Pt–Ru/C or Pt–Ru–Ni/C catalyst as the working electrode with an area of 0.0706 cm^2 was 10 μg (28 $\mu g_{metal}\ cm^{-2}$). CO was adsorbed on the surface of the Pt–Ru/C or Pt–Ru–Ni/C catalyst at 0.08 V by bubbling CO gas through the 0.5 mol L^{-1} H_2SO_4 solution for 25 min. CO dissolved in the solution was subsequently removed by bubbling argon gas of high purity for 35 min, keeping the potential also at 0.08 V. The potential was then cycled at a scanning rate of 0.02 V s^{-1} from 0.05 to 1.2 V for two oxidation and reduction cycles.

2.3. Physical measurements

2.3.1. X-ray diffraction (XRD)

XRD analysis was carried out for the catalysts with a D/max-rB (Japan) diffractometer using a Cu Kα X-ray source operating at 45 kV and 100 mA. The XRD patterns were obtained at a scanning rate of 4° min^{-1} with an angular resolution of 0.05° of the 2θ scan.

2.3.2. Energy dispersive analysis of X-ray (EDAX)

Chemical composition analysis by EDAX were performed with an EDAX Hitachi-S-4700 analyser associated to a scanning electron microscope (SEM, Hitachi Ltd. S-4700). Incident electron beam energies from 3 to 30 keV had been used. In all cases, the beam was at normal incidence to the sample surface and the measurement time was 100 s. All the EDAX spectra were corrected by using the ZAF correction, which takes into account the influence of the matrix material on the obtained spectra.

3. Results and discussion

3.1. Characterization of catalysts' X-ray diffraction

XRD patterns reveal the bulk structure of the catalyst and its support. Fig. 1 shows the XRD patterns of the Pt–Ru–Ni/C (curve A) and Pt–Ru/C (curve B) catalysts. It can be seen that the first peak located at a 2θ value of about 24.8° in the XRD pattern is referred to Vulcan XC-72 carbon support. The other

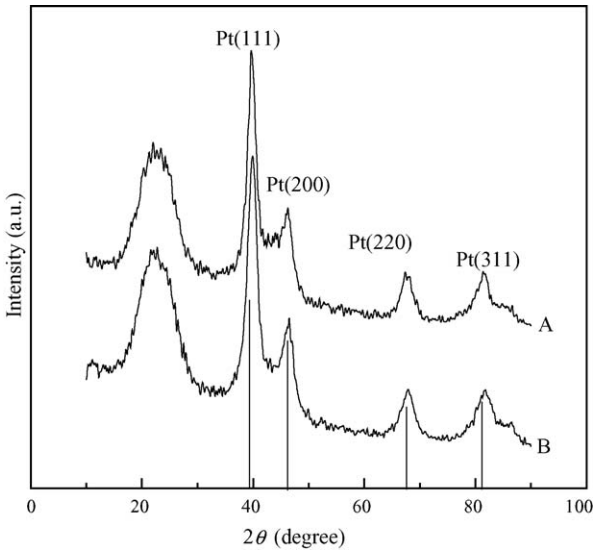

Fig. 1. XRD patterns of the Pt–Ru–Ni/C (A) and Pt–Ru/C (B) catalysts.

four peaks are characteristic of face centered cubic (fcc) crystalline Pt(JCPDS-ICDD, Card No. 04-802), corresponding to the planes (1 1 1), (2 0 0), (2 2 0) and (3 1 1) at 2θ values of about 39.8°, 46.5°, 67.8° and 81.2°, respectively, indicating that the alloy catalysts have principally single-phase disordered structures (i.e. solid solutions). Comparing with the reflections of pure Pt (cf. the vertical lines of Pt in Fig. 1, referring to the Joint Committee on Powder Diffraction Data (JCPDS-ICDD) database), the diffraction peaks for the Pt–Ru and Pt–Ru–Ni catalysts are shifted slightly to a higher 2θ values. The slight shifts of the diffraction peaks reveal the formation of an alloy involving the incorporation of Ru and Ni atoms into the fcc structure of Pt. It is important to note that no diffraction peaks, indicating the presence of either pure Ru and Ni or Ru-rich hexagonal close packed (hcp) phase, and Ni oxide, appear.

The lattice parameters of Pt–Ru and Pt–Ru–Ni catalysts, which reflect the formation of a solid solution and be calculated by using the Pt(1 1 1) crystal faces, are given in Table 1. The lattice parameters obtained for the Pt–Ru and Pt–Ru–Ni catalysts are smaller than those for Pt/C. In fact, the decrease in lattice parameters of the alloy catalysts reflects the progressive increase in the incorporation of Ru and Ni into the alloyed state. The average particle size d may be estimated from Pt(1 1 1) FWHM according to Debye–Scherrer formula[23,24]:

$$d = \frac{k\lambda}{\beta_{1/2}\cos\theta} \quad (1)$$

$$S = \frac{6000}{\rho d} \quad (2)$$

$$\rho_{Pt-Ru} = X_{Pt}\rho_{Pt} + X_{Ru}\rho_{Ru} \quad (3)$$

$$\rho_{Pt-Ru-Ni} = X_{Pt}\rho_{Pt} + X_{Ru}\rho_{Ru} + X_{Ni}\rho_{Ni} \quad (4)$$

where d is the average particle size (Å), λ the wavelength of X-ray (1.5406 Å), θ the angle, at which the peak maximum occurs, $\beta_{1/2}$ the width (in radians) of the diffraction peak at a half height, k a coefficient of 0.89–1.39 (0.9 here), ρ the density of Pt–Ru

Table 1
The lattice parameter, particle size and specific area of Pt–Ru–Ni/C and Pt–Ru/C catalysts

Catalysts	2θ (°)	d-Value (nm)	Lattice parameter (nm)	FWHM	Particle size (nm)	Specific area ($m^2\,g^{-1}$)
Pt/C	67.7	0.13873	0.3924	–	–	–
Pt–Ru/C	67.9	0.13794	0.3901	1.869	4.5	74.1
Pt–Ru–Ni/C	67.9	0.13791	0.3900	1.908	4.4	71.8

or Pt–Ru–Ni alloy, ρ_{Pt} the density of Pt metal (21.4 g cm^{-3}), ρ_{Ru} the density of Ru metal (12.3 g cm^{-3}), ρ_{Ni} the density of Ni metal (8.9 g cm^{-3}) and X_{Pt}, X_{Ru} and X_{Ni} are the weight percent of Pt, Ru and Ni, respectively, in the catalysts.

Table 1 gives the calculated average particle size and specific surface area of the catalysts according to their highest diffraction peaks of Pt(1 1 1). The particle size and specific surface area of the Pt–Ru/C and Pt–Ru–Ni/C catalysts are almost the same.

3.2. EDAX measurement

Chemical compositions of the Pt–Ru–Ni/C and Pt–Ru/C catalysts were determined by EDAX analysis. Fig. 2 shows EDAX patterns of the Pt–Ru–Ni/C (A) and Pt–Ru/C (B) catalysts. Typical values of the composition analysis of them are shown in Table 2.

The EDAX analysis shows that the determined composition is quite similar to the theoretical one. H_2PtCl_6, $RuCl_3$ and $NiCl_2$ as precursors were entirely reduced to Pt, Ru and Ni metals, respectively. The results are similar to those of the measurement of the filtrate collected during washing the catalysts' precipitate.

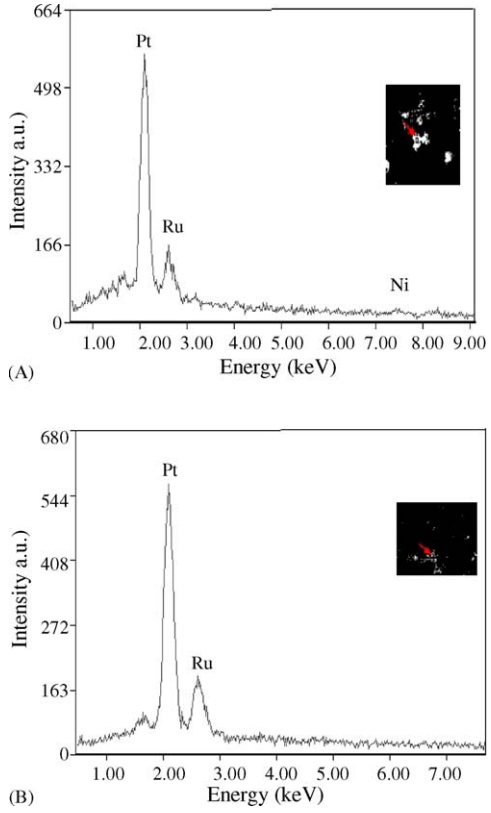

Fig. 2. EDAX patterns of the Pt–Ru–Ni/C (A) and Pt–Ru/C (B) catalysts.

Table 2
The atomic composition of Pt–Ru–Ni/C and Pt–Ru/C catalysts (at.%)

Catalysts	Nominal content			Determined by EDAX		
	Pt	Ru	Ni	Pt	Ru	Ni
Pt–Ru/C	50	50	–	56.3	43.7	–
Pt–Ru–Ni/C	60	30	10	63.2	30.1	6.7

3.3. The electrochemically active specific area of the catalysts

Fig. 3 shows the cyclic voltammograms on the Pt–Ru–Ni/C (A) and Pt–Ru/C (B) catalysts for CO oxidation in a solution of 0.5 mol L^{-1} H_2SO_4 at 25 °C.

The electrochemically active specific area (S_{EAS}) of the catalyst is calculated by using the following Eq. (5) [25,26] and the cyclic voltammetry curves of CO adsorption- and desorption-

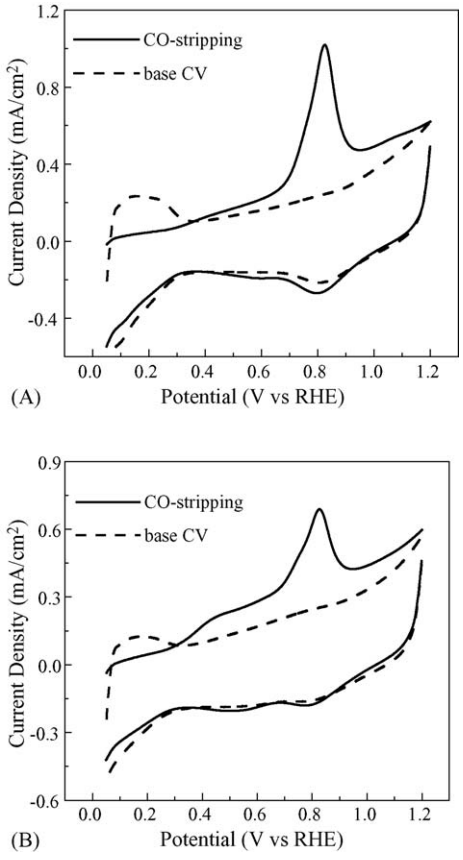

Fig. 3. Cyclic voltammograms for CO electrooxidation on the Pt–Ru–Ni/C (A) and Pt–Ru/C (B) catalysts in an Ar-saturated solution of 0.5 mol L^{-1} H_2SO_4 at 25 °C. Scan rate: 0.02 V s^{-1} (the data are derived from the glassy carbon based electrode measurements).

electrooxidation

$$S_{EAS} = \frac{Q_{CO}}{G \times 420} \quad (5)$$

where Q_{CO} is the charge for CO desorption-electrooxidation in microcoulomb (μC) G represents the summation of Pt + Ru or Pt + Ru + Ni metals' loading (μg) in the electrode, and 420 is the charge required to oxidize a monolayer of CO on the catalyst in $\mu C\,cm^{-2}$.

The electrochemically active specific areas of the Pt–Ru–Ni/C and Pt–Ru/C catalysts are 67.7 and 64.5 $m^2\,g^{-1}$, respectively, which are almost the same.

3.4. The electrochemical activity of the catalysts

Fig. 4 shows the cyclic voltammograms on the Pt–Ru–Ni/C (A) and Pt–Ru/C (B) catalysts with a solution of 0.5 mol L^{-1} CH_3CH_2OH and 0.5 mol L^{-1} H_2SO_4 at 25 °C. The performance of the Pt–Ru/C catalyst is the best among the Pt–Ru/C catalysts prepared by the same method and from the same precursors. A lot of work has been focused on the ethanol oxidation with Pt–Ru electrocatalysts [27–31]. Generally accepted ethanol oxidation behaviors on Pt–Ru are as follows. Similarly to methanol, the first step of the oxidation of ethanol is the cleavage of O–H bond, forming ethoxy species CH_3CH_2O. Further transformation of ethoxy species gives acetaldehyde CH_3CHO, which then can be oxidized by numerous reactions, forming acetate ion CH_3COO^-, acetone CH_3COCH_3, crotonaldehyde $CH_3CH{=}CHCHO$, acetyl CH_3CO, methane, other hydrocarbons, carbonate ion CO_3^{2-}, CO and CO_2. These reactants and reaction intermediates are adsorbed on the catalyst surface at lower potentials. When Ru–OH is generated by dissociative adsorption of H_2O on the catalyst surface, ethanol oxidation proceeds. However, the strong adsorption of OH on the catalyst surface at higher potentials inhibits further oxidation of ethanol, thus ethanol oxidation peaks are observed during positive potential scanning. When the potential scanning is reversed, the strongly adsorbed OH is reduced with the potential lowering. Then ethanol oxidation occurs again, thus its oxidation peaks are observed during negative potential scanning as shown in Fig. 4. It can be seen from Fig. 4 that the onset potential of a current rise for ethanol electrooxidation on the Pt–Ru–Ni/C catalyst corresponds to that on the Pt–Ru/C catalyst, i.e. about 0.55 V. The potential for ethanol electrooxidation, at which the peak current occurs is 0.92 V (versus RHE), and the peak current density is 13.8 mA cm^{-2} during positive potential scanning on the Pt–Ru–Ni/C catalyst as shown by curve A. The peak potential and the peak current density on the Pt–Ru–Ni/C catalyst are about 0.77 V (versus RHE) and 12.8 mA cm^{-2}, respectively, during its reverse scanning. The peak potential for ethanol electrooxidation and the peak current density on the Pt–Ru/C catalyst are about 0.91 V (versus RHE) and 9.8 mA cm^{-2}, respectively, during positive potential scanning as shown by curve B. The peak potential and the peak current density for the Pt–Ru/C catalyst are about 0.77 V (versus RHE) and 7.7 mA cm^{-2}, respectively, during its reverse scanning. The peak potential for the Pt–Ru–Ni/C catalyst during potential scanning is higher than that for the Pt–Ru/C catalyst. But the peak current density for the Pt–Ru–Ni/C catalyst is 4.0 mA cm^{-2} higher than that for the Pt–Ru/C catalyst. So, the performance of the Pt–Ru–Ni/C catalyst for ethanol electrooxidation is much better than that of the Pt–Ru/C catalyst. Furthermore, curves A and B are superposed at low potentials (0.05–0.45 V). It shows that the active sites and the specific area of the Pt–Ru/C and Pt–Ru–Ni/C catalysts are the same. This area is the same as electrochemically active specific surface area calculated with CO adsorption and oxidation. It can be seen from the above results that the performance of Pt–Ru–Ni/C catalyst is better than that of the Pt–Ru/C catalyst, mainly due to the improving effect of Ni in Pt–Ru/C catalyst for ethanol electrooxidation.

The activities of the catalysts for ethanol electrooxidation measured by steady-state current densities at a constant potential were used to compare the performance of the Pt–Ru–Ni/C and Pt–Ru/C electrocatalysts. Fig. 5 shows the current densities measured at a constant potential jumping from 0.1 to

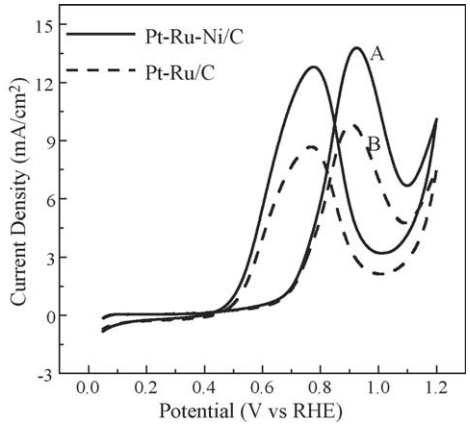

Fig. 4. Cyclic voltammograms of ethanol electrooxidation in an Ar-saturated solution of 0.5 mol L^{-1} CH_3CH_2OH and 0.5 mol L^{-1} H_2SO_4 at 25 °C on the Pt–Ru–Ni/C (A) and Pt–Ru/C (B) catalysts. Scan rate: 0.02 V s^{-1} (the data are derived from the glassy carbon based electrode measurements).

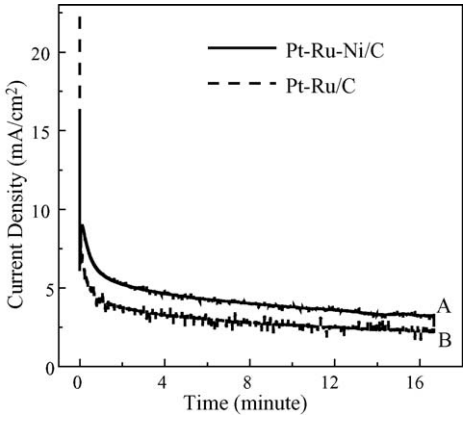

Fig. 5. Chronoamperometric curves of ethanol electrooxidation in an Ar-saturated solution of 0.5 mol L^{-1} CH_3CH_2OH and 0.5 mol L^{-1} H_2SO_4 at 25 °C on the Pt–Ru–Ni/C (A) and Pt–Ru/C (B) catalysts. Potential jumps from 0.1 to 0.8 V (the data are derived from the glassy carbon based electrode measurements).

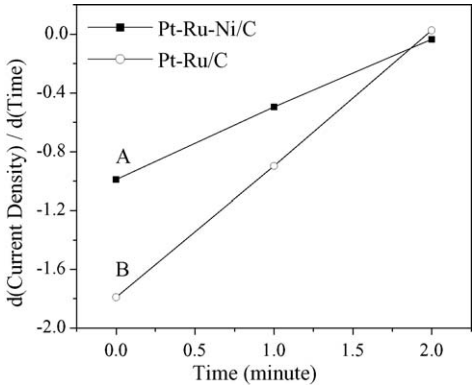

Fig. 6. d*i*/d*t* (normalized scale) against *t* plots from *t* = 0 to *t* = 2 min for Pt–Ru/C catalysts with or without addition of nickel. Slopes: 0.48 for Pt–Ru–Ni/C (A) and 0.88 for Pt–Ru/C (B) catalysts (the data are derived from the glassy carbon based electrode measurements).

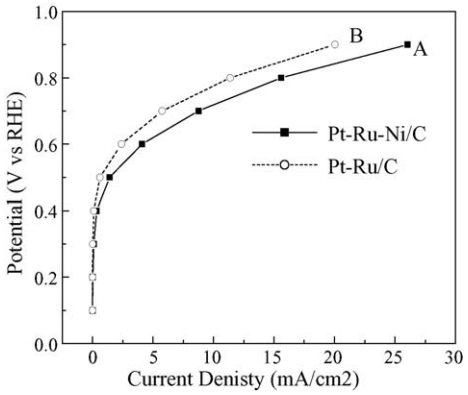

Fig. 7. Anodic polarization curves for the Pt–Ru–Ni/C and Pt–Ru/C electrodes in an Ar-saturated solution of 0.5 mol L^{-1} CH_3CH_2OH and 0.5 mol L^{-1} H_2SO_4 at 25 °C (the data are derived from half-cell measurements.).

0.8 V in an Ar-saturated solution of 0.5 mol L^{-1} CH_3CH_2OH and 0.5 mol L^{-1} H_2SO_4 at 25 °C. The initial high current corresponds mainly to double-layer charging. The currents decay with time in a parabolic style and reach an apparent steady state within 500 s. It can be seen that the current density of ethanol electrooxidation on the Pt–Ru–Ni/C catalyst is higher than that on the Pt–Ru/C catalyst at the same potentials, i.e. the activity of the Pt–Ru–Ni/C catalyst is better. The results are similar to those of cyclic voltammetry measurement.

Fig. 6, representing a d*i*/d*t* = *f*(*t*) plot (normalized scale) at small time values, allows the evaluation of the initial poisoning rate for the Pt–Ru–Ni/C or the Pt–Ru/C catalyst during the electrooxidation of ethanol. By comparing the two slopes, the greater the slope is, the easier the initial poisoning of the electrode surface is. It is clear that added nickel leads to less poisoning, since the experimental slope with added nickel is lower by a factor of 1.8, compared to that obtained without the addition of nickel, that is, 0.48 and 0.88, respectively.

There is electron transfer from nickel to platinum in Pt–Ni and, probably, from ruthenium to platinum in Pt–Ru, in agreement with the electronegativity series for Ni, Ru and Pt, i.e. 1.91, 2.2 and 2.28, respectively. The electron transfer may contribute to the decay of Pt–CO binding energy and enhance the formation of intermediates from ethanol electrooxidation. Furthermore, the surface layer containing both $Ni(OH)_2$ and NiOOH is formed on the Pt–Ru–Ni particles. The Ni hydroxide layer has some favorable properties, such as proton and electronic conductivities, and well protects the bulk from corrosion under ethanol electrooxidation conditions [13]. Such a hydroxide layer on Pt–Ru–Ni alloy may display high catalytic activity with respect to ethanol electrooxidation due to oxygen-containing species formed on the catalyst, and such species transform CO-like poisoning species on Pt into CO_2, leaving the active sites on Pt for further adsorption and oxidation of ethanol molecules. The obtained results indicate that the addition of Ni into Pt–Ru catalysts can significantly improve the electrode performance for ethanol electrooxidation.

3.5. Measurement of half cell

Fig. 7 shows a comparison of anodic polarization curves for the Pt–Ru–Ni/C (A) and Pt–Ru/C (B) electrodes in Ar-saturated 0.5 mol L^{-1} CH_3CH_2OH and 0.5 mol L^{-1} H_2SO_4 at 25 °C. The two electrodes were prepared and measured with the same method except that the catalysts used in electrodes were different. The electrode with Pt–Ru–Ni/C catalyst shows lower polarization than that with Pt–Ru/C catalyst. For example, the overpotential of the Pt–Ru–Ni/C electrode is 0.71 V (versus RHE) at 10 mA cm^{-2}, which is 60 mV lower than that of the Pt–Ru/C electrode. The result indicates that the Pt–Ru–Ni/C catalyst exhibits a higher catalytic activity for ethanol electrooxidation. The results are similar to those of cyclic voltammetric and chronoamperometric measurements.

The promoting effect attributable to the addition of nickel to platinum–ruthenium on the electrooxidation of ethanol is particularly significant at low potentials, as can be clearly seen in Fig. 8, which shows the ratio of the current densities, measured under quasisteady state conditions, with and without the addition of nickel, as a function of the oxidation potential (data taken from Fig. 7). This figure shows that the addition of nickel gives a maximum ratio at a potential of about 0.3 V (versus RHE), at

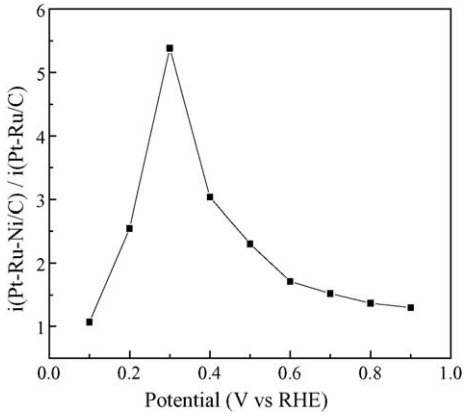

Fig. 8. Ratio of the current densities of ethanol oxidation recorded on the Pt–Ru–Ni/C and Pt–Ru/C electrodes as a function of the potential (the data are derived from half-cell measurements).

which the current density for ethanol oxidation (measured under quasisteady state conditions) is enhanced by a factor of 5.4.

4. Conclusions

Electrocatalytic activity of the Pt–Ru–Ni/C catalyst, formed by reduction with $NaBH_4$ of the inorganic salt precursors, was investigated with respect to the electrooxidation of ethanol in H_2SO_4 solution. The experimental data reported in this paper indicate that the performance of the Pt–Ru–Ni/C catalyst for ethanol electrooxidation is better than that of the Pt–Ru/C catalyst due to the promoting function of Ni. The CO-tolerance performance during ethanol electrooxidation of the Pt–Ru–Ni/C is better than that of Pt–Ru/C. By comparing the $i(E)$ curve recorded on the Pt–Ru–Ni/C electrode with the $i(E)$ curve recorded on the Pt–Ru/C electrode at $E = 0.3$ V (versus RHE), the current density of ethanol oxidation is enhanced by a factor of 5.4 in the presence of nickel (Fig. 8). Study of the mechanism is in progress.

Acknowledgements

This work is supported financially by Heilongjiang Natural Science Foundation (B0201) and Harbin Institute of Technology (HIT.2002.39).

References

[1] H. Uchida, Y. Mizuno, M. Watanabe, J. Electrochem. Soc. 149 (2002) A682.
[2] W.C. Choi, J.D. Kim, S.I. Woo, Catal. Today 74 (2002) 235.
[3] Z.B. Wang, G.P. Yin, P.F. Shi, Carbon 44 (2006) 133.
[4] C. Lamy, E.M. Belgsir, J.-M. Leger, J. Appl. Electrochem. 31 (2001) 799.
[5] G.A. Camara, R.B. de Lima, T. Iwasita, Electrochem. Commun. 6 (2004) 812.
[6] C. Lamy, S. Rousseau, E.M. Belgsir, C. Coutanceau, J.-M. Leger, Electrochim. Acta 49 (2004) 3901.
[7] V. Pacheco Santos, G. Tremiliosi-Filho, J. Electroanal. Chem. 554/555 (2003) 395.
[8] F.J. Rodriguez-Nieto, T.Y. Morante-Catacora, C.R. Cabrera, J. Electroanal. Chem. 571 (2004) 15.
[9] L.H. Jiang, G.Q. Sun, Z.H. Zhou, W.J. Zhou, Q. Xin, Catal. Today 93–95 (2004) 665.
[10] A. Oliveira Neto, E.G. Franco, E. Arico, M. Linardi, E.R. Gonzalez, J. Eur. Ceram. Soc. 23 (2003) 2987.
[11] M. Gotz, H. Wendt, Electrochem. Acta 43 (1998) 3637.
[12] U.A. Paulus, A. Wokaun, G.G. Scherer, T.J. Schmidt, V. Stamenkovic, V. Radmilovic, N.M. Markovic, P.N. Ross, Oxygen reduction on carbon-supported Pt–Ni and Pt–CO alloy catalysts, J. Phys. Chem. B 106 (2002) 4181.
[13] K.W. Park, J.H. Choi, B.K. Kwon, S.A. Lee, Y.E. Sung, H.Y. Ha, S.A. Hong, H.S. Kim, A. Wieckowski, J. Phys. Chem. B 106 (2002) 1869.
[14] T.C. Deivaraj, W.X. Chen, J.Y. Lee, J. Mater. Chem. 13 (2003) 2555.
[15] K.W. Park, J.H. Choi, Y.E. Sung, J. Phys. Chem. B 107 (2003) 5851.
[16] H. Yang, C. Coutanceau, J.-M. Leger, N. Alonso-Vante, C. Lamy, J. Electroanal. Chem. 576 (2005) 305.
[17] V. Stamenkovic, T.J. Schmidt, P.N. Ross, N.M. Markovic, J. Phys. Chem. B 106 (2002) 11970.
[18] H. Yang, W. Vogel, C. Lamy, N. Alonso-Vante, J. Phys. Chem. B 108 (2004) 11024.
[19] J.-F. Drillet, A. Ee, J. Friedemann, R. Kotz, B. Schnyder, V.M. Schmidt, Electrochim. Acta 47 (2002) 1983.
[20] T. Toda, H. Igarashi, H. Uchida, M. Watanabe, J. Electrochem. Soc. 146 (1999) 3750.
[21] Z.B. Wang, G.P. Yin, P.F. Shi, Acta Chimica Sinica 63 (2005) 1813.
[22] T.J. Schmidt, H.A. Gasteiger, G.D. Stab, P.M. Urban, D.M. Kolb, R.J. Behm, J. Electrochem. Soc. 145 (1998) 2354.
[23] C.Z. He, H.R. Kunz, J.M. Fenton, J. Electrochem. Soc. 144 (1997) 970.
[24] L. Giorgi, A. Pozio, C. Bracchini, R. Giorgi, S. Turtu, J. Appl. Electrochem. 31 (2001) 325.
[25] A. Pozio, M. de Francesco, A. Cemmi, F. Cardellini, L. Giorgi, J. Power Sources 105 (2002) 13.
[26] C.L. Green, A. Kucernak, J. Phys. Chem. B 106 (2002) 1036.
[27] S.A. Kirillov, P.E. Tsiakaras, I.V. Romanova, J. Mol. Struct. 651–653 (2003) 365.
[28] A.V. Tripkovic, K.Dj. Popovic, J.D. Lovic, Electrochim. Acta 46 (2001) 3163.
[29] C. Lamy, A. Lima, V. LeRhun, F. Delime, C. Coutanceau, J.-M. Leger, J. Power Sources 105 (2002) 283.
[30] N. Fujiwara, K.A. Friedrich, U. Stimming, J. Electroanal. Chem. 472 (1999) 120.
[31] A. Yee, S.J. Morrison, H. Idriss, J. Catal. 186 (1999) 279.